

HIGH RESOLUTION 11.6 μm IMAGES OF THE CENTRAL 1 PARSEC OF THE GALACTIC CENTER WITH A NEW 58 x 62 Si:Ga ARRAY CAMERA

DANIEL Y. GEZARI
*NASA/Goddard Space Flight Center
Infrared Astrophysics Branch - Code 685
Greenbelt, MD 20771*

1. Introduction

Seeing-limited 11.6- μm images of the central 1 parsec (~ 20 arcsec) of the Galactic Center have been obtained with a new 58 x 62 pixel Si:Ga array camera system. Previous array observations (Gezari *et al.* 1985) were used to derive the color temperature structure of the region. This higher spatial resolution work resolves new structure, showing a strong similarity (and notable discrepancies) between the 11.6- μm emission and the 6-cm continuum VLA maps (c.f., Morris and Yusef-Zadeh 1986) and closely correlated Brackett α infrared array images (Forrest *et al.* 1986). Careful comparison of the dust and ionized gas emission distributions shows most of the compact 11.6- μm dust sources are displaced from the gas peaks.

2. Instrumentation and Observations

The new array camera system uses a 58 x 62 pixel Si:Ga (gallium-doped silicon) DRO (direct readout) photoconductor detector array sensitive from 5 - 17 microns, manufactured by Hughes/Santa Barbara Research Center (SBRC). The array and optical assembly are cooled to 10 Kelvin. An off-axis parabolic mirror optical design incorporating a 5 - 14 μm circular variable filter (CVF) wheel and cold aperture stop produces diffraction-limited images with undetectable distortion and good background suppression. The camera system electronic architecture is divided into three sub-systems: 1) high speed analog front end, including 2-channel low noise preamp module, timing generator, low noise bias power supplies, 2) two 16 bit, 3 microsec/conversion analog-to-digital converters interfaced to a Mercury ZIP 3216 arithmetic array processor, and 3) a LSI 11/73 camera control and data analysis computer. A complete description of the array camera system is presented by Gezari *et al.* (1988).

The nearly diffraction limited images ($\lambda/D = 0.8$ arcsec FWHM) were made at the NASA Infrared Telescope Facility (IRTF) at Mauna Kea on the night of 15 March 1988. The background-limited observational system NEFD = 0.05 Jy $\text{min}^{-1/2}\text{pixel}^{-1}$ with 0.26 arcsec pixels, a CVF filter wheel spectral bandwidth $\Delta\lambda/\lambda = 4\%$, and operating at a frame rate of 30 Hz. Image quality was seeing-limited at about 1.0 arcsec (FWHM). The image in Figure 1 was obtained in a single 1-minute integration.

3. Discussion

The nearly diffraction limited 11.6 μm image (Figure 1) reveals new extended infrared source structure strikingly similar to the 6-cm continuum map (Yusef-Zadeh 1986) with the same resolution (Figure 2a). The details of the extended dust emission are now resolved, and appear to have nearly identical clumpy structure as the ionized gas. The 6-cm and 11.6 μm point sources are coincident at the positions of IRS 1, 2 and 9, and are slightly displaced at IRS 10 and 6.

However, there are significant discrepancies in the positions of the other bright emission peaks near Sgr A*. There is a tendency for the ionized gas source to lie closer to Sgr A* than the corresponding dust peaks. This effect is apparent in two ways: a) The ionized gas emission shows a strong double-peaked source ~ 4 arcsec southwest of Sgr A* where the southern peak coincides with IRS 2, but there is no comparable 11.6 μm counterpart to the northern peak (the position of the near infrared source IRS 13). Similarly, the strong 6-cm peak ~ 2 arcsec south of Sgr A* has no strong 11.6 μm counterpart (see Figure 2b). b) In IRS 10 and 6 the Br α and 6-cm peak is displaced toward Sgr A* from the 11.6 μm dust peak, although the IRS 10 dust feature correlates with other compact 6-cm structure.

Considering the high relative positional accuracy of the array images (± 0.1 arcsec) and the quality of the ionized gas data, the positional displacements observed are significant. The enhanced ionized gas brightness near Sgr A* can be interpreted as emission from regions which are relatively hotter and depleted of dust than the outlying adjacent 11.6 μm bright regions. The effects could be attributed to the influence of a central luminosity source near the position of Sgr A*. The coincidence of the 6-cm and 11.6 μm features at IRS 1, 2, 9 and 10 is suggestive of embedded luminosity sources at those positions. The new data provide additional constraints on models for the structure and heating of the inner galactic center region.

W. J. Forrest, M. A. Shure, J. L. Pipher, and C. E. Woodward 1986, Proc. Townes Symposium on the Galactic Center, (American Institute of Physics, 155), 127.

D. Y. Gezari, R. Tresch-Feinberg, G. G. Fazio, W. Hoffmann, I. Gatley, G. Lamb, P. Shu, and C. McCreight 1985, Ap. J., 299, 1007.

D. Y. Gezari, W. Folz, L. Woods, and J. Wooldridge 1988, Proc. S.P.I.E. Symposium, 973.

M. Morris and F. Yusef-Zadeh 1986, Proc. Townes Symposium on the Galactic Center (American Institute of Physics, 155), 153.

F. Yusef-Zadeh 1986 (private communication).

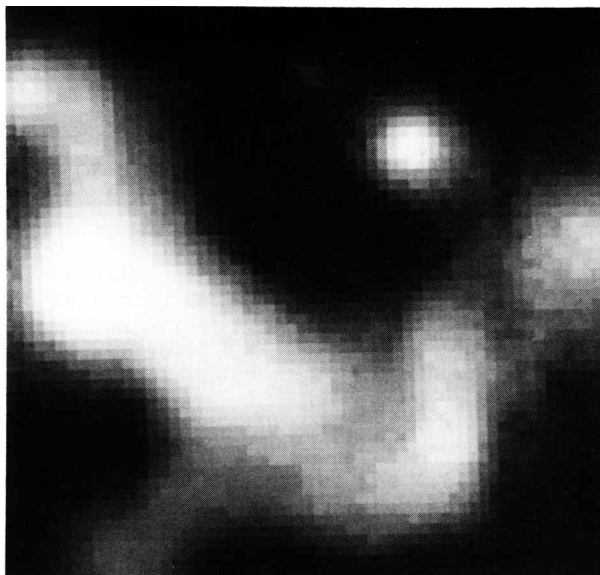


Figure 1: $11.6\ \mu\text{m}$ array camera image of the central 1 parsec (~ 20 arcsec) of the galactic center, obtained in a 1 min integration centered on the position of Sgr A*. The bright compact IRS sources are identified in Figure 2(b). This 1 arcsec resolution image reveals extended infrared source structure strikingly similar to the Brackett α and 6-cm continuum VLA distributions, with notable discrepancies in the positions of the bright peaks.

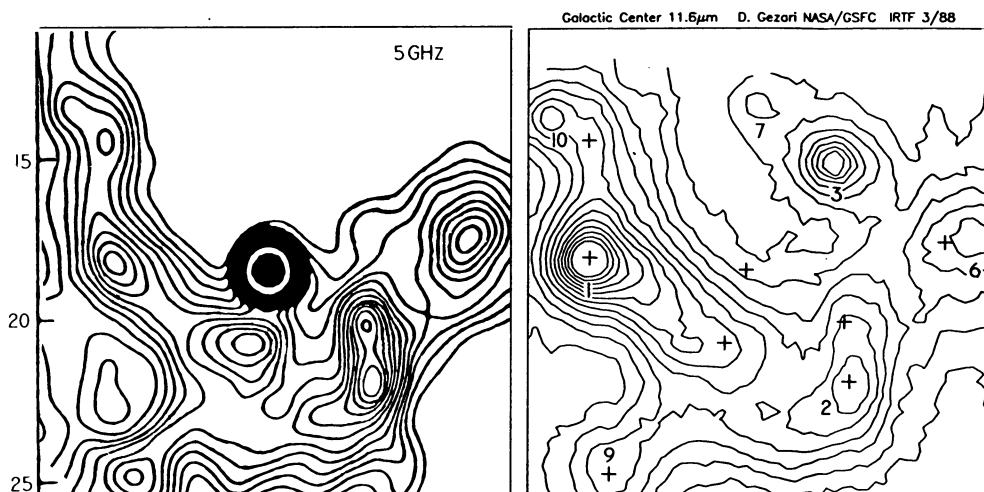


Figure 2a (left): 5 GHz radio continuum map of the central parsec of the Galactic Center (F. Yusef-Zadeh 1986, private communication). The bright central object is the Sgr A* non-thermal source. Note the bright double source about 4 arcsec SW of Sgr A*, and the peak 2 arcsec S of Sgr A*, referred to in the text. **Figure 2b (right):** Contour map of the $11.6\ \mu\text{m}$ emission made from five co-added 1 minute integrations like the image presented in Figure 1. The IRS sources are numbered and the positions of Sgr A* and the radio continuum peaks from Figure 2a are shown with crosses. Note the radial displacement of the $11.6\ \mu\text{m}$ and radio continuum peaks at IRS 10 and IRS 6 away from Sgr A*, the relative weakness of the $11.6\ \mu\text{m}$ emission at the two 6-cm peaks closest to Sgr A*, and the coincidence of the dust and gas peaks at IRS 1, IRS 2, and IRS 9.